Original Article

Radiation and energy balance on a hillslope forest: horizontal versus slope-parallel installation of radiometer

WANG Xing-chang [1,2] https://orcid.org/0000-0002-6502-1422; e-mail: xcwang_cer@nefu.edu.cn

LIU Fan [1,3] https://orcid.org/0000-0002-2567-9174; e-mail: liufan@sjziam.ac.cn

WANG Chuan-kuan [1,2*] https://orcid.org/0000-0003-3513-5426; e-mail: wangck-cf@nefu.edu.cn

*Corresponding author

1 Center for Ecological Research, Northeast Forestry University, Harbin 150040, China

2 Key Laboratory of Sustainable Forest Ecosystem Management – Ministry of Education, Northeast Forestry University, Harbin 150040, China

3 Key Laboratory of Agricultural Water Resources, Center for Agricultural Resources Research, Institute of Genetics and Developmental Biology, Chinese Academy of Sciences, Shijiazhuang 050021, China

Abstract: Radiation is a major driver to the carbon, water, and energy exchanges of an ecosystem. For local radiation balance measurements, one essential question is whether the measurement systems should be installed horizontally or parallel to inclined slope surface. With a case study over a temperate deciduous forest on a moderate inclined (9°) northwest-facing slope, we quantified the slope effect on net radiation (R_n) and its components and the energy balance closure measured by an eddy covariance (EC) system. Compared with the slope-parallel radiometer, the horizontal sensor overestimated the incident solar radiation (SR) by 7%, the incoming photosynthetically active radiation (PAR) by 1.5%, and the incoming near-infrared radiation (NIR) by 10%; while underestimated the reflected shortwave radiation (SR) by 4% and NIR by 5%. The influence of radiometer-orientation on incoming longwave radiation (LR) was about 3%, while that on outgoing LR was negligible. Summing all these components, horizontal sensor overestimated the R_n by 9%. Converting the horizontally-measured incident radiation to slope-surface reduced a half of the biases on incoming SR and R_n. Measuring the R_n with slope-parallel radiometer and correcting the slope-effect on horizontally-measured incident SR improved the energy balance ratio (EBR) by 8% and 5%, respectively. A mini-review indicated that, the horizontal sensor underestimated (overestimated) the EBR on north-facing (south-facing) slopes in temperate zone in the Northern Hemisphere, with an inclination angular sensitivity of EBR as high as 1.17% per degree of inclination angle. We recommend measuring radiations on inclined terrains with slope-parallel radiometers, or correcting at least for the incident SR in energy balance studies.

Keywords: Radiation; Sloping terrain; Energy balance closure; Eddy covariance

1 Introduction

The climate is fundamentally determined by the magnitude and distribution of the radiation budget of the Earth (Trenberth et al. 2009). Radiation budget

determines the net energy into an ecosystem, thus is a prerequisite factor for ecosystem processes such as the carbon and water exchanges between the atmosphere and ecosystem (Bala et al. 2007). Therefore, accurately measuring radiation components on diverse surfaces is fundamental to quantify and simulate climate change and ecosystem carbon, water, and energy budgets (Bai and Zong 2021; Xu et al. 2021; Yan et al. 2021).

Radiometer is the most common instrument for measuring local radiation budget (Olmo et al. 1999; Wohlfahrt et al. 2016), which is often installed horizontally due to the operational advantages (Whiteman et al. 1989). On mountainous regions that cover one quarter of the Earth's land surface (Barry 2008), however, horizontally-installed radiometers may be inappropriate (Olmo et al. 1999; Wohlfahrt et al. 2016), because their hemispherical viewing angles are not parallel to the radiation received or reflected by the underlying surfaces (Hoch and Whiteman 2010). Topography may influence radiation components (e.g., visible, near-infrared, and longwave radiations) (Matzinger et al. 2003; Holst et al. 2005) to some degree, depending upon the geographical location and topographical geometry. Nevertheless, few studies assess effects of sensor-orientation on radiation components on non-flat terrain, although they have contrasting environmental biophysical meanings.

The eddy-covariance (EC) method has been used to directly measure the net exchange of carbon, water and energy between the atmosphere and ecosystem (Baldocchi et al. 2001; Aubinet et al. 2012). In the FLUXNET (Schimel et al. 2015), most anemometers for the EC systems and accompanied radiation sensors were installed horizontally, even over sloping terrains. One key correction conducted for the turbulent flux calculation on sloping terrains is the tilt-correction, i.e., rotating the anemometer's coordinate framework to perpendicular to the mean streamlines, usually using planar-fit or double rotation (Aubinet et al. 2012; Leuning et al. 2012). However, the radiation measurements are generally not corrected to the same plane as does the turbulent energy flux. As a result, the net or available radiation is often out of phase with the turbulent energy flux [the sum of sensible (H) and latent heat (LE) fluxes], leading to biased energy balance closure (EBC) (e.g., Serrano-Ortiz et al. 2016; Wohlfahrt et al. 2016). There are two potential solutions to this problem: (1)

measuring the net all-waveband radiation (R_n) with a slope-parallel instrumentation (Matzinger et al. 2003; Wohlfahrt et al. 2016), or (2) converting the horizontally-measured R_n into a slope-parallel framework by mathematical transformations (Hammerle et al. 2007; Hiller et al. 2008; Zitouna-Chebbi et al. 2012; Serrano-Ortiz et al. 2016; Wohlfahrt et al. 2016), which is like the "tilt-correction" in the EC method. The effect of these approaches, however, needs more assessment (Serrano-Ortiz et al. 2016; Moderow et al. 2021). First, the turbulent heat fluxes are perpendicular to the streamlines of the airflow, may be not the exactly local terrain-inclination (Sun 2007). Second, converting the horizontally-measured radiations to sloping coordinates needs to know its direct and diffuse components, which are often poorly modeled in the literature (e.g., Wohlfahrt et al. 2016). Comparisons between these approaches will not only help correct historical data using better models, but also provide an appropriate method to guide future studies.

The radiation energy balance is mainly composed of four components, i.e., incoming and outgoing shortwave (or solar radiation, 300–2800 nm, SR) and longwave (4.5–42 μm, LR) radiations, respectively, which have different effects on the climate and ecosystem processes. Moreover, many land-surface models (e.g., Sellers et al. 1996; Liang et al. 2003) divide the SR into visible (or photosynthetically active radiation, PAR, 400–700 nm) and near-infrared radiation (NIR, 700–2800 nm) due to their contrasting biophysical meanings (Weiss and Norman 1985). Therefore, examining sensor-orientation effects on radiation components of different wavelengths would be useful for understanding and modeling ecological processes. To date, however, no corrections for topographic effects on radiation fully account for the radiation components. For example, Serrano-Ortiz et al. (2016) quantified the slope-effect on the R_n without its components. Holst et al. (2005) reported that the differences between the reflected SR measured with slope-parallel and horizontal sensors were relatively small compared with the incoming SR, but the deviations between both sensors were sometimes up to 20%. However, studies rarely reported the topographic effects on PAR, NIR and LR components.

In this paper, we compared the R_n and its components as well as the albedos measurements between horizontal and slope-parallel radiometers,

and assessed their effects on the EBC in a temperate deciduous forest on a sloping terrain. Our objectives were to: (1) quantify the sensor-orientation effect on radiation components (i.e., PAR, NIR and LR); (2) compare direct measurements of radiation with slope-parallel sensors versus slope-corrected radiation values measured with horizontal sensors; and (3) explore the effect of the general patterns of sensor-orientation on the EBC across sites with various slope azimuths and inclination angles by literature synthesis.

2 Materials

2.1 Site description

The study was conducted at the Maoershan Forest Ecosystem Research Station of Northeast Forestry University, Heilongjiang Province, Northeast China. The climate is continental monsoon, with mean (2008–2018) annual air temperature of 2.0°C, and mean annual precipitation of 676 mm (Liu et al. 2021a). A 48-m-high EC tower was set up at the low-part of the south-west sidewall of a northeast-southwest valley with ~2 km wide and ~240 m deep (Fig. 1). The forest around the tower was a 70-year-old temperate broadleaved deciduous stand with a 20-m canopy height. The mean inclination angle of the

slope around the tower is ~9° (Wang et al. 2015), and the slope azimuth is northwest (~296°). The mean maximum leaf area (semi-surface leaf area) index of the stand, measured with the litterfall collection method from nine 20 m × 30 m permanent plots, was 6.3 ± 0.8 (SD) m^2 m^{-2} in 2016 (Liu et al. 2021b).

2.2 Instrumentation and data collection

The R_n and its components were determined by duplicate sensors in two configurations (Fig. 2), one horizontal and the other parallel to the surface (Serrano-Ortiz et al. 2016). For each configuration, the R_n and energy balance of four radiation components, i.e., incoming shortwave (SR) and longwave (LR) versus outgoing shortwave (SR) and longwave (LR) radiation, were measured with the CNR4 (Kipp & Zonen, the Netherland). In addition, the incoming and outgoing PAR were also measured with a pair of PQS1 sensors (Kipp & Zonen, the Netherland), one facing up and the other facing down with both vertical and slope-normal orientations. All radiometers were installed at 48 m height on supporting booms pointing to the up-slope direction. Because of the slope-angle increase along the upslope direction, the 9°-inclination of the slope-parallel sensors at 48 m height at the slope-toe is roughly parallel to the angle of the measurement point to the
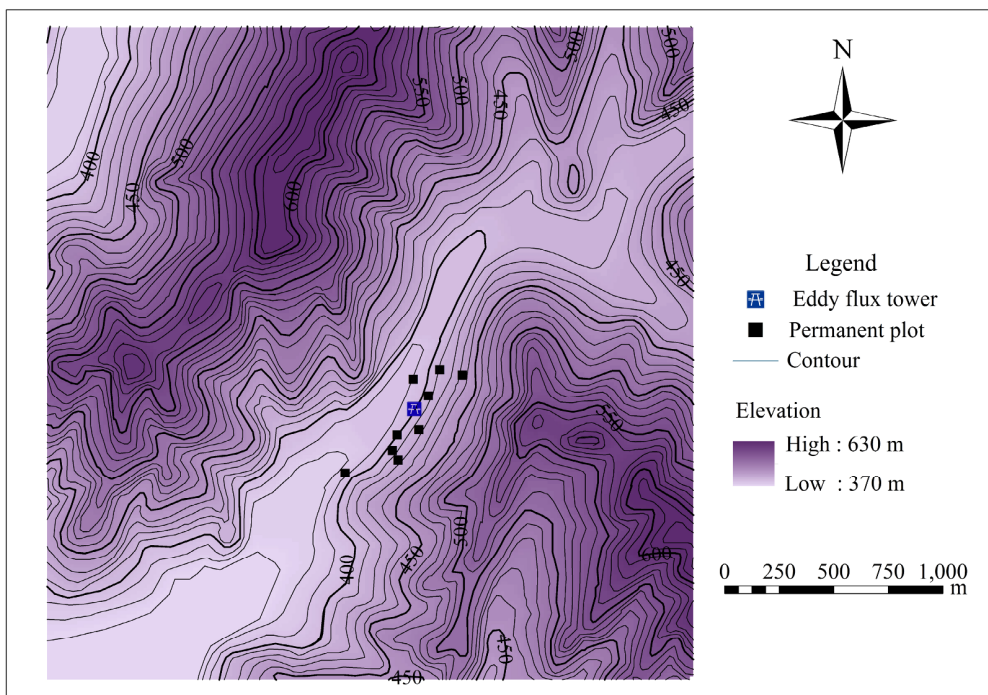

Fig. 1 Contour map of the study site at the Maoershan eddy flux tower site.

ridge of the slope relative the horizontal, which pre
vent significant illumination of the downward sensors
at low solar elevations in the morning. A side-by-side
comparison of each paired-radiometer was conducted
for six months before the measurements started to
ensure that the subsequent inter-comparisons
between the orientations were minimally affected by
any drift. Linear models with the ordinary least
square regression (all deviation of the slope with one
≤ 1.8%, offset ≤ 1.8 W m⁻², R^2 ≥ 0.997, and RMSE ≤
7.5 W m⁻²) were used to remove the relative biases of
all slope-parallel radiometers with reference to the
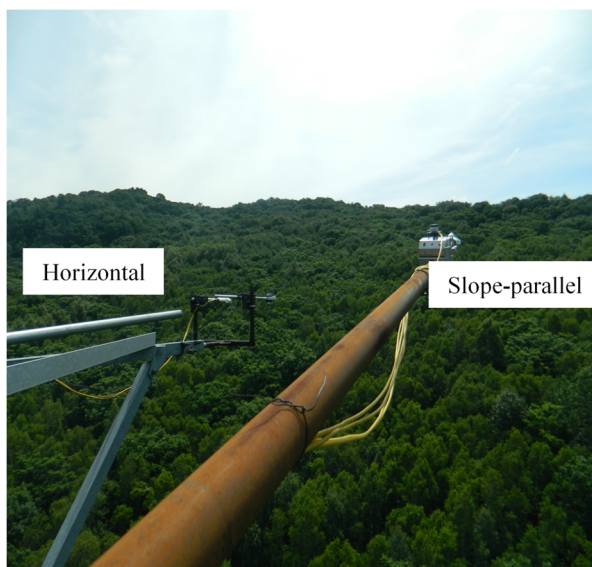horizontal counterparts.

Fig. 2 Photograph of installations of radiation sensors.

To calculate the available energy, four soil heat-
flux plates (HFP01SC, Hukseflux, Delft, Netherlands)
were installed parallel to the ground surface at the 8-
cm depth (Serrano-Ortiz et al. 2016). To calculate the
energy storage above the heat-flux plates, two pairs of
soil temperature probes (TCAV, Campbell Scientific,
USA) were installed at the 2- and 6-cm depth,
respectively; and two TDRs for measuring soil water
content (CS616, Campbell Scientific, USA) were
inserted at the 4-cm depth (Serrano-Ortiz et al. 2016).

The turbulent fluxes were measured with the EC
method. An open-path EC system was installed at 36
m height, with the CSAT3 (Campbell Scientific Inc,
Logan, Utah, USA) horizontally and the LI-7500 (Li-
Cor Inc, Lincoln, NE, USA) mounted vertically. The
original data were recorded at a frequency of 10 Hz
with a datalogger (CR3000, Campbell Scientific Inc,
USA).

3 Data Processing

The analyses were based on the data from the
whole leaf-on season (from May 3 to October 10,
2016) with the data coverage of 100% for the
radiation and 67% for the turbulent energy fluxes.

3.1 Radiation

The budget for each radiation component (net
SR, PAR, NIR, and LR) was calculated as the
difference between the incoming and outgoing
components. The NIR was calculated by subtracting
the PAR from the SR. The PAR in photon flux density
(µmol photons m⁻² s⁻¹) was converted to energy flux
density (W m⁻²) using conversion factors of 0.2195 J
µmol⁻¹ for incoming PAR and 0.2072 J µmol⁻¹ for
outgoing PAR (Ross and Sulev 2000).

To compare between the two ways for correcting
the topographic effect on radiation balance i.e.,
directly measuring with a slope-parallel sensor versus
converting radiation measured with a horizontal
sensor to the slope-surface, the horizontally measured
radiation was rotated to the slope coordinate with
various methods. For completeness, the detailed
slope-correction methods were given in Appendixes 1-
3. For this conversion, the diffuse SR, outgoing SR,
incoming and outgoing LR were treated as isotropic
based on our results. Considering the accuracy is not
sensitive to model-selection (Appendix 4), we adopted
a series of common empirical equations (Liu and
Jordan 1963; Spitters 1986; Alados and Alados-
Arboledas 1999). Briefly, the horizontally measured
incoming SR was partitioned into solar beam (direct)
and diffuse radiation using the method by Spitters et
al. (1986), then the direct radiation was rotated
perpendicular to the slope surface (Liu and Jordan
1963), and finally the slope-normal incoming SR was
obtained by summing the simulated slope-normal
direct incoming SR and the diffuse incoming SR. The
diffuse component of incoming PAR from diffuse
incoming SR was estimated by the method proposed
by Alados and Alados-Arboledas (1999).

3.2 Energy balance closure

The H and LE fluxes were calculated with the flux
measurement procedures (Aubinet et al. 2012),
including despiking, time-lag removing, planar-fit tilt
correction, frequency response correction, WPL

correction, and quality control (Wang and Wang 2016). The EBC was formularized by the first law of thermodynamics as:

$$H + \text{LE} = R_\text{n} - G_0 - S - Q \tag{1}$$

The left-hand side of Eq. (1) is the turbulent energy fluxes (sum of the H and LE measured with the EC system), whereas the right-hand represents the available energy, including the net radiation (R_n), the soil heat flux (G_0, calculated by summing the heat fluxes measured at the 8-cm depth of the mineral soil and the energy stored in the layer above the heat-flux plates), the heat storage (S) between the soil surface and the EC system (36 m), and the sum of additional energy sources and sinks (Q). In this study, S was neglected in comparison between sensor-orientations as did at most sites due to impractical measurements (Wilson et al. 2002; Stoy et al. 2013), and Q was neglected because of its small magnitude (Jarvis et al. 1997). We assumed that ignoring S and Q would not influence the inter-comparison of the EBC between the sensor-orientations because they were neglected for both methods.

The EBC at the half-hour scale was evaluated by the linear regression coefficients (slope and intercept) of the major axis (MA) regression – an approach suitable as a consistency test between two variables or methods (Wang et al. 2016; Warton et al. 2006), between the turbulent energy and the available energy (Wilson et al. 2002). The EBC for the whole leaf-on season between horizontal and slope-parallel radiometers was assessed by the energy balance ratio (EBR):

$$\text{EBR} = \Sigma(H + \text{LE})/\Sigma(R_\text{n} - G_0) \tag{2}$$

Such bulk integration method minimized the effect of missing terms (S and Q), because the energy storage would cancel out at long-term scales (Jarvis et al. 1997; Stoy et al. 2013), as the temperature at the
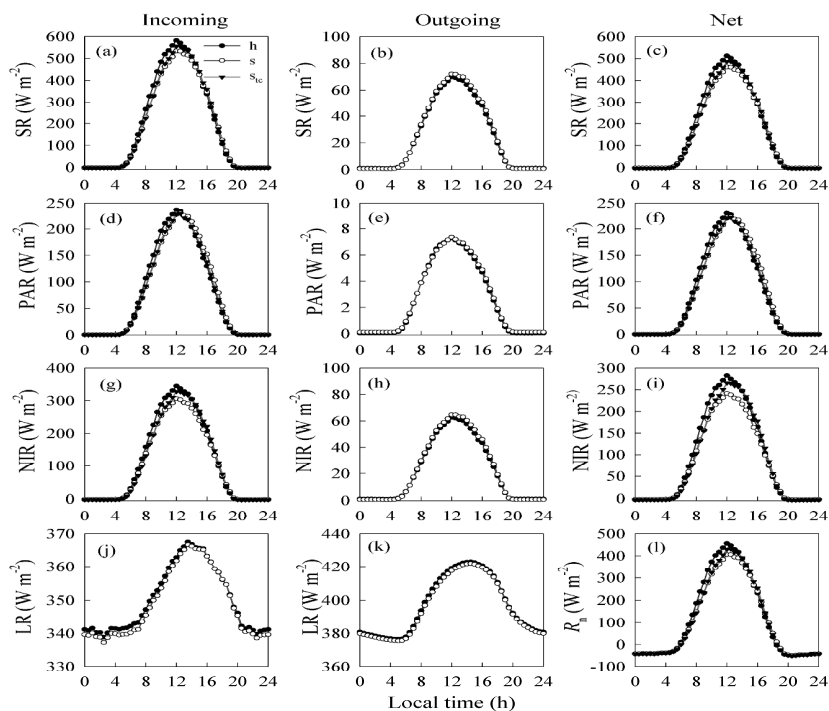

Fig. 3 Mean diurnal variations in radiation components measured with horizontal and slope-parallel sensors in the leaf-on season (May 3 – October 10, 2016). The left, middle, and right panels are incoming, outgoing, and net radiations, respectively. (a) – (c) solar radiation (SR), (d) – (f) photosynthetically active radiation (PAR), (g) – (i) near-infrared radiation (NIR), (j) – (k) longwave radiation (LR), and (l) net radiation (R_n). The legends h, s and s_tc represent horizontal and slope-parallel sensors and tilt-corrected horizontal sensors, respectively.

beginning (May 3) and the end (October 10) of the study period was close to each other.

4　Results

4.1　Diurnal variations in radiation components

For the whole leaf-on season, the sensor-orientation effect on the diurnal variations in radiation was more dramatic for incoming SR versus outgoing SR, while generally negligible for both incoming and outgoing LR (Fig. 3). The slope-parallel sensor reduced the SR in the morning and early afternoon by ~50 W m⁻² (Fig. 3a), but increased outgoing SR by ~1 W m⁻² (Fig. 3b), leading to a reduced and lagged net SR (Fig. 3c). Further partitioning the SR into the PAR and NIR broadbands indicated that the time-lag in incoming SR was mainly caused by the incoming PAR component (Fig. 3d), but the amplitude reduction was largely derived from the

incoming NIR (Fig. 3g). Both outgoing PAR and NIR were slightly enhanced by the slope-parallel sensors (Figs. 3e and 3h), leading to slightly lower amplitudes of the net PAR and NIR for the sloping-sensors (Figs. 3f and 3i). The slope-parallel sensors only slightly reduced and lagged both incoming and outgoing LR (Figs. 3j and 3k). The horizontal radiometer overestimated the R_n in late-morning and midday by ~50 W m^{-2}, but underestimated the R_n in the afternoon by ~20 W m^{-2}.

4.2 Slope effect on radiation components

Compared with slope-parallel sensors, horizontal sensors overestimated the R_n, net SR, incoming SR, net NIR, and incoming NIR by 9% (Fig. 4a), 8% (Fig. 4b), 7% (Fig. 4c), 14% (Fig. 4h), and 10% (Fig. 4i), respectively, but underestimated the outgoing SR and NIR by 4% and 5%, correspondingly (Figs. 4d and 4j).
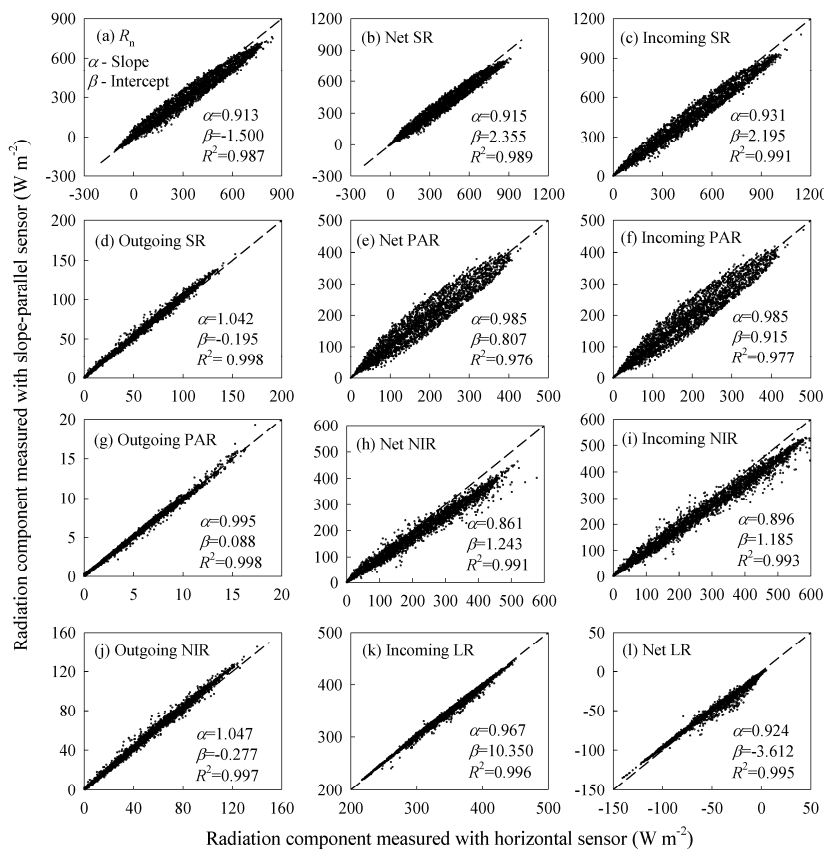
Horizontal sensors overestimated the net PAR and incoming PAR only by 1.5% (Figs. 4e and 4f), but time-lagged much larger than the incoming NIR, as indicated by the wider oval shape of the scatter plots. Horizontal sensors underestimated incoming LR by ~3%, with an intercept of 10.35 W m^{-2} (Fig. 4k), whereas that for outgoing LR was negligible (slope = 0.997, intercept = 0.133 W m^{-2}, R^2 = 1.000). Therefore, horizontal sensors underestimated the net LR by 8%, with an intercept of −3.613 W m^{-2} (Fig. 4l).

Converting the incoming SR and its components measured with horizontal sensors to the slope surface generally reduced the differences in incoming radiations and R_n between horizontal versus slope-parallel sensors (Fig. 5). The "tilt-correction" for incoming SR and R_n reduced the corresponding errors by roughly 51% and 47%, respectively. And the "tilt-correction" reduced the error in the incoming NIR by 28%, while slightly changed the error in the incoming PAR. However, compared with the direct method (measuring with slope-parallel sensors), the slope-corrections overestimated the incoming SR, R_n and incoming NIR correspondingly by 3%, 5% and 8%, but underestimated incoming PAR by 2%.

4.3 Energy balance closure

Measuring the R_n with slope-parallel sensors and correcting slope-effect measured with the horizontal sensors both improved the agreement between the turbulent energy (H+LE) and the available energy (R_n-G_o) (Figs. 6a and 6b). The maximum improvement (> 60 W m^{-2}) occurred at around 11:00. The slope-parallel radiometer and topography-correction also reduced the diurnal hysteresis loop (Figs. 6c and 6d), but slope-parallel radiometer resulted in a better EBC (a slope closer to 1)

Fig. 4 Major-axis regressions of radiation components measured with horizontal versus slope-parallel sensors in the leaf-on season (May 3 – October 10, 2016). (a) Net radiation (R_n), (b) net solar radiation (SR), (c) incoming SR, (d) outgoing SR, (e) net photosynthetically active radiation (PAR), (f) incoming PAR, (g) outgoing PAR, (h) net near-infrared radiation (NIR), (i) incoming NIR, (j) outgoing NIR, (k) incoming longwave radiation (LR), and (l) net LR. The slope (α), intercept (β), and R^2 are given for each radiation component. The dotted line represents 1:1 line.
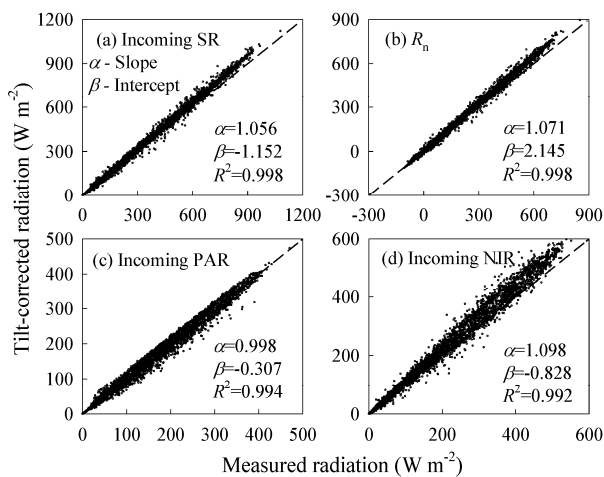
Fig. 5 Major-axis regressions of measured versus tilt-corrected radiation components in a slope-parallel coordinate framework in the leaf-on season (May 3 – October 10, 2016). (a) Incoming solar radiation (SR), (b) net radiation (R_n), (c) incoming photosynthetically active radiation (PAR), and (d) incoming near-infrared radiation (NIR).

Table 1 Summary of the major axis regression forced through the origin (zero intercept) between the turbulent energy (H + LE) and the available energy (R_n − G_0) measured with horizontal and slope-parallel sensors and tilt-corrected horizontal sensors.

Sensor orientation	R^2	Slope	EBR
Horizontal	0.856	0.678	0.773
Surface-parallel	0.882	0.757	0.857
Tilt-corrected	0.883	0.722	0.825

Notes: R_n, G_0, H, and LE are net radiation, soil heat, sensible heat, and latent heat fluxes, respectively. EBR is energy balance ratio [Eq. (2)]. Both regressions are highly significant (N = 52203, P < 0.001).

versus the tilt-correction. The MA regressions showed that, the slope-parallel radiometer improved the explained variance (R^2) by 2.6%, and increased the slope forced through the origin for the half-hour measurements by 7.9% (from 0.678 to 0.757, Table 1). Slope-corrected R_n improved the MA slope by a less amount of 4.4%. The slope-parallel radiometer and the simple slope-correction increased the EBR by 8.4% and 5.2%, respectively.

5 Discussion

5.1 Radiometer-orientation effect on radiation components in the mountainous terrain

We found that the radiometer-orientation effect on incoming SR was greater than on incoming LR (Fig. 3), consistent with previous studies (Holst et al.

2005; Wohlfahrt et al. 2016). However, further component partitioning showed that radiometer-orientation had a contrasting effect on daily means and time-lags of the PAR versus the NIR wavebands (Fig. 3). At our site, the slope-parallel radiometer caused a large phase-shifting in incoming PAR due to the large azimuth angle (116° from the south), but only 1.5% reduction in the sums of incoming PAR (Fig. 4f) mainly due to canceling effect between the morning down-regulation and afternoon up-regulation introduced by the small inclination angle (9°). In contrast, it resulted in 10% reduction in the sum of incoming NIR, but only produced a small phase-shifting in its diurnal pattern (Fig. 3g). Such a diurnal asymmetry for incoming SR and its components should be considered in the simulations of radiation budget, carbon and water cycling on complex terrains (Wang et al. 2005), because of the different ecological functions of PAR and NIR. Compared with sunny slopes, the reduction in NIR but not PAR on the shady slope indicated that the thermal effect of NIR (and thus suppressed temperature increase and water consumption) would be reduced but kept similar PAR for photosynthesis. This slope effect of SR components partly interprets that why the water conditions in temperate shady slope is better than that in sunny slope. In addition, the phase-shifting in PAR indicated that a potential influence in the light response curve of net ecosystem exchange of CO_2 and thus the light use efficiency. This direct effect on radiation and indirect effect on water conditions of slope should be considered in forest management particularly silviculture.

The small difference in outgoing SR (4%) between the horizontal and slope-parallel sensors (Fig. 4d) led to a marginal effect on R_n (< 1%), because of the small SR albedo (~0.15) caused by the dense canopy. It is reasonable to assume that the outgoing SR is isotropic for most EC sites. However, the effect could increase with increasing inclination angle (Holst et al. 2005).

The sensor-orientation effect on LR is quite different from that on SR. The slightly decrease in incoming LR in the morning may due to the west side-wall of the valley decreasing the angular exposure to the radiating sky of the inclined sensor. During the afternoon and the nighttime, however, the warmer opposite slope over-compensated the decreased sky view factor, and thus caused slightly more LR for the slope-parallel than the horizontal sensors (Whiteman
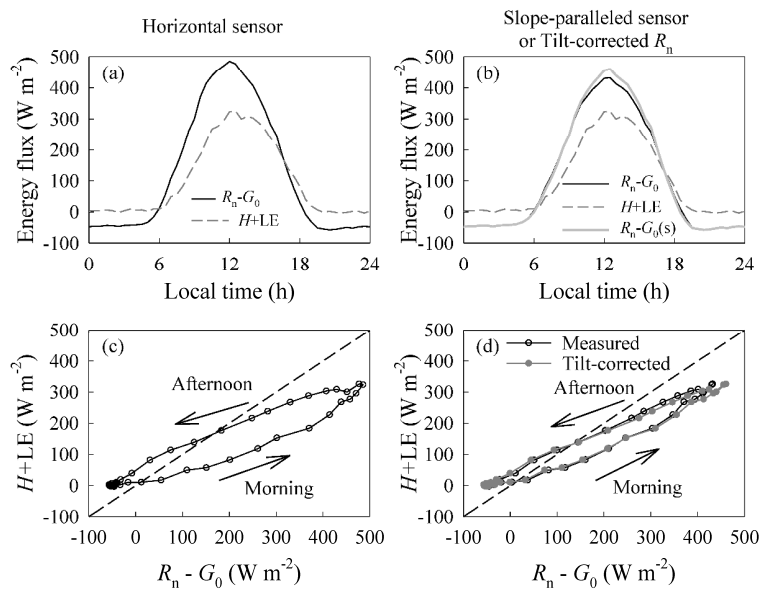
Fig. 6 Mean diurnal patterns of the turbulent energy (H + LE) and the available energy (R_n – G_o) measured with horizontal sensors (a) and with slope-parallel sensors or slope-corrected horizontal sensors (b), and the corresponding hysteresis curves (c, d) during the leaf-on season (May 3 – October 10, 2016). R_n, G_o, H, and LE are net radiation, soil heat, sensible heat, and latent heat fluxes, respectively.

et al. 1989; Matzinger et al. 2003; Hoch et al. 2011). The little difference in outgoing LR between the two sensor-orientations in this study and the literature (Holst et al. 2005; Whiteman et al. 1989) suggested a negligible effect of sensor-orientation on outgoing LR.

The phase-shifts in the slope-corrected SR and/or R_n relative to the horizontal measurements depend on the nature of slope aspect (Hoch and Whiteman 2010). The phase-shifts to a postnoon maximum often occur on west-facing slopes (Fig. 2; Matzinger et al. 2003; Hiller et al. 2008; Serrano-Ortiz et al. 2016; Wohlfahrt et al. 2016), while the shifts to a prenoon peak occur on east-facing slopes (Whiteman et al. 1989; Holst et al. 2005; Hammerle et al. 2007). Since the incoming SR dominates the R_n (Fig. 2; Matzinger et al. 2003; Hoch and Whiteman 2010), and is the component most affected by slope (Fig. 4), accounting for the topographic effect on incoming SR may yield reasonable results, but likely introduce bias on steep slopes (Serrano-Ortiz et al. 2016).

The "tilt-corrected" horizontal measurements produced reasonable result for incoming SR, and PAR as well as R_n, but relatively poor for NIR (Figs. 3 and 5). This might be attributed to: (1) The simple empirical models of diffuse radiation correlation had a typical error of 20%–30% (Jacovides et al. 2006;

Gueymard and Ruiz-Arias 2016), which was large for accurate modeling purpose (e.g., Wohlfahrt et al. 2016). (2) Converting the diffuse radiation to the slope ignored the different fractions of the sky and the surrounding terrain, and the isotropic assuming for both sky diffuse and reflected radiation (Liu and Jordan 1963) was too simple to accurately simulate its diurnal patterns (Yang 2016). (3) Using the constant conversion factors of 0.2195 J μmol^{-1} for incoming PAR (Ross and Sulev 2000) across all sky conditions might also introduce uncertainty at the half-hour time-scale. And separating the proportion of PAR from the modeled diffuse SR using empirical model could ensure the compatibility of PAR and SR, but would introduce further uncertainties by error propagation. We had shown similar results between various partitioning equations of diffuse PAR, and they resulted in similar results (Appendix 4). (4) Calculating NIR by subtracting PAR from SR might introduce further uncertainties to NIR by error propagation. Despite of these errors, our findings implied a strong necessary to partition SR into PAR and NIR. In-situ measuring the diffuse radiation would help produce good agreement between simulation and measurement (Whiteman et al. 1989).

5.2 Radiometer-orientation effect on the energy balance closure in the mountainous terrain

The energy imbalance at forest sites seems to be a universal problem. Our best estimate of EBR for the leaf-on season (0.86), after accounting the orientation-effect on the R_n, is very similar to that reported in the FLUXNET synthesis (Stoy et al. 2013): 0.84 for 173 sites, 0.83 for 88 forest sites; while the yearly EBR at the former without accounting the influence of topography on R_n in 2011 (0.69; Wang and Wang 2016) is close to the mean at the deciduous forest sites (0.70; Stoy et al. 2013). The question we would ask is what are the potential error sources of the energy imbalance. Measuring R_n with slope-parallel radiometer (Serrano-Ortiz et al. 2016;

Wohlfahrt et al. 2016) or correcting only incoming SR (Hammerle et al. 2007; Hiller et al. 2008) might both reduce the diurnal hysteresis and improve the balance between the available energy and the turbulent energy, but we found the former was better (Fig. 6 and Table 1). Besides, other potential contributors to the EBR imbalance may include exclusion of the storage flux term (Leuning et al. 2012), underestimation of low frequency covariance by insufficient average period (Finnigan et al. 2003), influence of advections or mesoscale circulations (Rotach et al. 2014) induced by the landscape scale heterogeneity of topography or vegetation (Stoy et al. 2013), or/and the underestimation of the vertical velocity fluctuation that affects the estimation of the turbulent energy fluxes (Frank et al. 2013). In forest ecosystems, however, the biomass energy storage is difficult to measure; the G_o contributes only minor to the overall available energy compared with R_n because of the dense canopy.

Is there any key factor driving the slope effect on EBR across sites? To address this question, we compiled all published and our data (Table 2). We found that the slope effect was slope-aspect-dependent. Theoretically, in the northern hemisphere, horizontal sensors overestimate the available energy of the ecosystem on north-facing slopes (Table 1 and Zitouna-Chebbi et al. 2012), but underestimate it on south-facing slopes. Correcting slope effect systematically reduced the EBR on south-facing slopes, but increased it on north-facing slopes (Table 2). This contrasting slope-aspect effect between south- and north-facing slopes agrees well with the theoretical inference (Zitouna-Chebbi et al. 2012; Serrano-Ortiz et al. 2016). However, accounting the topographic effect on R_n or only on incoming SR may either increase or decrease the slope of ordinary least square regression, which might be interfered by the large decrease in the intercept of the linear regression (Table 2). We recommend assessing the EBC either using the regression slope by forcing the regression line through the origin (Leuning et al. 2012), or using

Table 2 Comparisons of the effect of correcting horizontally measured radiations on energy balance closure across sites in the literature. The Δslope, ΔIntercept, and ΔR^2 represent the changes in the slope, intercept, and R^2 of the ordinary least square regression of the turbulent energy flux (H + LE) on the available energy (R_n – G_o) after accounting the slope-effect, respectively. The EBR is the energy balance ratio calculated by Eq. (5). The values at the Kamech A and Kamech C sites were estimated based on the changes in net radiation. All dataset had a measurement period of one to five months. The values are either cited from the literature or recalculated form the half-hour data shared with the authors (notes with*).

Site	Lat. (°N)	Vegetation	Slope aspect	Inclination angle	ΔSlope	ΔIntercept (W m⁻²)	ΔR^2	ΔEBR	Tilt-corrected EBR	Reference
Kaserstattalm, Austria	47.13	Grassland	ESE (116°)	24°	−0.05	−38	0.14	−0.25	0.73	Hammerle et al. 2007
Crap Alv, Switzerland*	48.58	Grassland	SSW (205°)	25°	0.08	−60	0.17	−0.24	0.84	Hiller et al. 2008
Venosta Valley, Italy*	46.48	Grassland	WSW (255°)	24°	0.03	-9	0.08	−0.34	0.98	Wohlfahrt et al. 2016
Sierra Nevada National Park, Spain*	36.97	Grassland	SW (227°)	10°	−0.08	−28	0.19	−0.19	1.32	Serrano-Ortiz et al. 2016
Kamech catchment A, Tunisia	36.88	Cropland	SE	8°				−0.11	0.91	Zitouna-Chebbi et al. 2012
Kamech catchment C, Tunisia	36.88	Cropland	NW	5°				0.12	0.82	Zitouna-Chebbi et al. 2012
Bílý Kříž, Czech Republic	49.51	Forest	SSW	−13°	−0.11		0.04	−0.13	0.71	McGloin et al. 2018
Rájec, Czech Republic	49.44	Forest	NEE	5°	0.01		0	0	0.73	McGloin et al. 2018
Štítná, Czech Republic	49.03	Forest	WSW	−10°	0.05		0.02	−0.07	0.61	McGloin et al. 2018
Ritten/Renon, Italy	46.58	Forest	S	−11°	0.07	1	0	−0.08	1.16	Moderow et al. 2021
Maoershan, China	45.40	Forest	WNW (296°)	9°	0.08	−2	0.04	0.08	0.86	This study

the EBR (Stoy et al. 2013).

Furthermore, we found a significant linear relationship of ΔEBR with the inclination angle by pooling the data across the 11 sites (Fig. 7), which had great implications on the EBR over sloping terrains. First, the regression slope indicated a sensitivity of (1.07±0.22)% of the EBR per degree of inclination angle, which was high for the global mean EBR of 0.84 (Stoy et al. 2013). Second, the near-zero intercept (1.84 ± 3.29) suggested an unbiased estimate on flat terrains. Third, the high R^2 (0.69) and relatively low RMSE (8.35%) of the linear model suggested its potential use for approximate corrections at other sites. The regression can be improved if the deviation of exact south or north of the aspect, the differences in treatment of intercept (forcing the regression line through the origin or not) were considered. Because of the high sensitivity of EBR to inclination angle across the sites (c.f. Wohlfahrt et al. 2016), we recommend measuring the R_n over sloping terrains with slope-parallel sensors; otherwise, at least correcting the incoming SR. The slope-correction of radiation might be hindered by rolling terrain, but we emphasize the basic assumption of uniform terrain for eddy covariance is also violated in very complex terrains. Encouragingly, Wohlfahrt et al. (2016) reported that accounting the spatial variability of inclination and aspect had similar effect in reducing the hysteresis and improving the agreement between available energy and the turbulent heat fluxes, as did the average inclination and aspect.

The aspect-dependent and the high inclination-angle sensitivity of slope effect on EBR also have
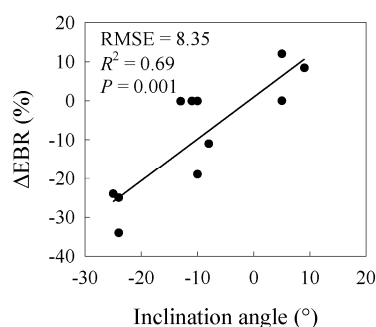

Fig. 7 Relationship between the change in energy balance ratio (ΔEBR) due to correcting the slope-effect on radiation with the inclination angle across 11 sites. The data are from Table 2. The inclination angle was set to be negative for south-facing slopes and positive for north-facing slopes, according to the directions of ΔEBR between the contrasting slope aspects.

implications for the eddy-flux corrections. Based on a detailed analyses of the uncertainties in available and turbulent energies, Twine et al. (2000) suggested adjusting the EBR to unit for calculating the energy and CO_2 fluxes. However, we argue that the correction of slope effect on EBR in mountainous forest sites must be taken into consideration before performing any correction of the energy imbalance (turbulent energy deficit or surplus) for evapotranspiration (Jung et al. 2010), LE (Jung et al. 2011), or CO_2 (Barr et al. 2006).

6 Conclusions

The effect of sensor-orientation on the diurnal variations in radiations was larger for incoming than outgoing radiations, and larger in SR than LR on the northwest-facing slope. The direct effect on radiation of slope and its subsequent influence on water conditions should be considered in forest management at least in temperate regions. Simple "tilt-correction" by converting the horizontally-measured incident radiation to the slope-coordinate only reduced a half of the biases in incoming SR and R_n, indicating such simple conversion schedule should be improved. Measuring R_n with the slope-parallel radiometer or correcting the slope-effect on horizontally-measured incoming SR consistently reduced the diurnal phase-lag of the sum of sensible and latent heat flux relative to the available energy, and improved the EBR by 8% and 5%, respectively. A linear model based on a literature survey suggests that the sensitivity of error in EBR caused by inclination is estimated as high as 1.17% per degree of inclination angle, suggesting that a "tilt-correction" of R_n for EBR is indispensable over sloping terrains. For the energy balance related studies, we recommend measuring radiations and albedos over inclined terrains with slope-parallel radiometers at mountainous forest terrains.

Electronic supplementary material: Supplementary material (Appendixes 1-4) is available in the online version of this article at https://doi.org/10.1007/s11629-022-7481-8.

References

Alados I, Alados-Arboledas L (1999) Direct and diffuse photosynthetically active radiation: measurements and modelling. Agr Forest Meteorol 93(1): 27-38. https://doi.org/10.1016/S0168-1923(98)00107-5

Aubinet M, Vesala T, Papale D (2012) Eddy covariance: a practical guide to measurement and data analysis. Springer.

Bai J, Zong X.(2021) Global solar radiation transfer and its loss in the atmosphere. Appl Sci-Basel 11(6): 2651. https://doi.org/10.3390/app11062651

Bala G, Caldeira K, Wickett M, et al. (2007) Combined climate and carbon-cycle effects of large-scale deforestation. P Natl Acad Sci USA 104(16): 6550-6555. https://doi.org/10.1073/pnas.0608998104

Baldocchi D, Falge E, Gu L, et al. (2001) FLUXNET: A new tool to study the temporal and spatial variability of ecosystem–scale carbon dioxide, water vapor, and energy flux densities. B Am Meteorol Soc 82(11): 2415-2434. https://doi.org/10.1175/1520-0477(2001)082<2415:FANTTS>2.3.CO;2

Barr AG, Morgenstern K, Black TA, et al. (2006) Surface energy balance closure by the eddy-covariance method above three boreal forest stands and implications for the measurement of the CO_2 flux. Agr Forest Meteorol 140(1): 322-337. https://doi.org/10.1016/j.agrformet.2006.08.007

Barry RG (2008) Mountain Weather and Climate 3e. Cambridge University Press.

Finnigan JJ, Clement R, Malhi Y, et al. (2003) A re-evaluation of long-term flux measurement techniques part I: averaging and coordinate rotation. Bound-Lay Meteorol 107(1): 1-48. https://doi.org/10.1023/A:1021554900225

Frank JM, Massman WJ, Ewers BE (2013) Underestimates of sensible heat flux due to vertical velocity measurement errors in non-orthogonal sonic anemometers. Agr Forest Meteorol 171-172: 72-81. https://doi.org/10.1016/j.agrformet.2012.11.005

Gueymard CA, Ruiz-Arias JA (2016) Extensive worldwide validation and climate sensitivity analysis of direct irradiance predictions from 1-min global irradiance. Sol Energy 128: 1-30. https://doi.org/10.1016/j.solener.2015.10.010

Hammerle A, Haslwanter A, Schmitt M, et al. (2007) Eddy covariance measurements of carbon dioxide, latent and sensible energy fluxes above a meadow on a mountain slope. Bound-Lay Meteorol 122(2): 397-416. https://doi.org/10.1007/s10546-006-9109-x

Hiller R, Zeeman MJ, Eugster W (2008) Eddy-covariance flux measurements in the complex terrain of an alpine valley in Switzerland. Bound-Lay Meteorol 127(3): 449-467. https://doi.org/10.1007/s10546-008-9267-0

Hoch SW, Whiteman CD (2010) Topographic effects on the surface radiation balance in and around Arizona's Meteor Crater. J Appl Meteorol Clim 49(6): 1114-1128. https://doi.org/10.1175/2010JAMC2353.1

Hoch SW, Whiteman CD, Mayer B (2011) A systematic study of longwave radiative heating and cooling within valleys and basins using a three-dimensional radiative transfer model. J Appl Meteorol Clim 50(12): 2473-2489. https://doi.org/10.1175/JAMC-D-11-083.1

Holst T, Rost J, Mayer H (2005) Net radiation balance for two forested slopes on opposite sides of a valley. Int J Biometeorol 49(5): 275-284. https://doi.org/10.1007/s00484-004-0251-1

Jacovides CP, Tymvios FS, Assimakopoulos VD, et al. (2006) Comparative study of various correlations in estimating hourly diffuse fraction of global solar radiation. Renew Energ 31 (15):2492-2504. https://doi.org/10.1016/j.renene.2005.11.009

Jarvis PG, Massheder JM, Hale SE, et al. (1997) Seasonal variation of carbon dioxide, water vapor, and energy exchanges of a boreal black spruce forest. J Geophysical Res-Atmos 102(D24): 28953-28966. https://doi.org/10.1029/97JD01176

Jung M, Reichstein M, Ciais P, et al. (2010) Recent decline in the global land evapotranspiration trend due to limited moisture supply. Nature 467(7318): 951-954. https://doi.org/10.1038/nature09396

Jung M, Reichstein M, Margolis HA, et al. (2011) Global patterns of land-atmosphere fluxes of carbon dioxide, latent heat, and sensible heat derived from eddy covariance, satellite, and meteorological observations. J Geophysical Res-Biogeo 116(G3): G00J07 https://doi.org/10.1029/2010JG001566

Leuning R, van Gorsel E, Massman WJ, et al. (2012) Reflections on the surface energy imbalance problem. Agr Forest Meteorol 156: 65-74. https://doi.org/10.1016/j.agrformet.2011.12.002

Liang S, Shuey CJ, Russ AL, et al. (2003) Narrowband to broadband conversions of land surface albedo: II. Validation. Remote Sens Environ 84(1): 25-41. http://doi.org/10.1016/S0034-4257(02)00068-8

Liu, BYH, Jordan RC (1963) The long-term average performance of flat-plate solar-energy collectors: With design data for the U.S., its outlying possessions and Canada. Sol Energy 7(2): 53-74. https://doi.org/10.1016/0038-092X(63)90006-9

Liu F, Wang X, Wang C, et al. (2021a) Environmental and biotic controls on the interannual variations in CO_2 fluxes of a continental monsoon temperate forest. Agr Forest Meteorol 296: 108232. https://doi.org/10.1016/j.agrformet.2020.108232

Liu F, Wang C, Wang X (2021b) Sampling protocols of specific leaf area for improving accuracy of the estimation of forest leaf area index. Agr Forest Meteorol 298-299: 108286. https://doi.org/10.1016/j.agrformet.2020.108286

Matzinger N, Andretta M, Van Gorsel E, et al. (2003) Surface radiation budget in an Alpine valley. Q J Roy Meteor Soc 129(588): 877-895. https://doi.org/10.1256/qj.02.44

Moderow U, Grünwald T, Queck R, et al. (2021) Energy balance closure and advective fluxes at ADVEX sites. Theor Appl Climatol 143(1): 761-779. https://doi.org/10.1007/s00704-020-03412-z

Olmo FJ, VidanJ, Foyon I, et al. (1999) Prediction of global irradiance on inclined surfaces from horizontal global irradiance. Energy 24(8):689-704. http://doi.org/10.1016/S0360-5442(99)00025-0

Ross J, Sulev M (2000) Sources of errors in measurements of PAR. Agr Forest Meteorol 100(2–3): 103-125. http://doi.org/10.1016/S0168-1923(99)00144-6

Rotach, Mathias W, Wohlfahrt G, et al. (2014) The world is not

flat: Implications for the global carbon balance. B Am Meteorol Soc 95 (7):1021-1028.
http://doi.org/10.1175/bams-d-13-00109.1

Schimel D, Pavlick R, Fisher JB, et al. (2015) Observing terrestrial ecosystems and the carbon cycle from space. Global Change Biol 21(5): 1762-1776.
http://doi.org/10.1111/gcb.12822

Sellers PJ, Randall DA, Collatz GJ, et al. (1996) A Revised Land Surface Parameterization (SiB2) for Atmospheric GCMS. Part I: Model Formulation. J Climate 9(4): 676-705.
http://doi.org/10.1175/1520-0442(1996)009<0676:arlspf>2.0.co;2

Serrano-Ortiz P, Sánchez-Cañete EP, Olmo FJ, et al. (2016) Surface-parallel sensor orientation for assessing energy balance components on mountain slopes. Bound-Lay Meteorol 158(3): 489-499.
http://doi.org/10.1007/s10546-015-0099-4

Spitters CJT (1986) Separating the diffuse and direct component of global radiation and its implications for modeling canopy photosynthesis Part II. Calculation of canopy photosynthesis. Agr Forest Meteorol 38(1-3): 231-242.
https://doi.org/10.1016/0168-1923(86)90061-4

Spitters CJT, Toussaint HAJM, Goudriaan J (1986) Separating the diffuse and direct component of global radiation and its implications for modeling canopy photosynthesis Part I. Components of incoming radiation. Agr Forest Meteorol 38(1-3): 217-229.
https://doi.org/10.1016/0168-1923(86)90060-2

Stoy, PC, Mauder M, Foken T, et al. (2013) A data-driven analysis of energy balance closure across FLUXNET research sites: The role of landscape scale heterogeneity. Agr Forest Meteorol 171: 137-152.
https://doi.org/10.1016/j.agrformet.2012.11.004

Sun J (2007) Tilt corrections over complex terrain and their implication for CO_2 transport. Bound-Lay Meteorol 124(2): 143-159.
https://doi.org/10.1007/s10546-007-9186-5

Trenberth KE, Fasullo JT, and Kiehl J (2009) Earth's global energy budget. B Am Meteorol Soc 90(3): 311-323.
https://doi.org/10.1175/2008BAMS2634.1

Twine TE, Kustas WP, Norman JM, et al. (2000) Correcting eddy-covariance flux underestimates over a grassland. Agr Forest Meteorol 103(3): 279-300.
https://doi.org/10.1016/S0168-1923(00)00123-4

Wang Q, Tenhunen J, Schmidt M, et al. (2005) Diffuse PAR irradiance under clear skies in complex alpine terrain. Agr Forest Meteorol 128(1-2): 1-15.
https://doi.org/10.1016/j.agrformet.2004.09.004

Wang X, Wang C (2016) Effects of coordinate rotations on eddy fluxes over a forest on a mountainous terrain in Northeast China. Chinese J Appl Ecol 27(9): 2779-2788. (In Chinese)
https://doi.org/10.13287/j.1001-9332.201609.012

Wang X, Wang C, Guo Q, et al. (2016) Improving the CO_2 storage measurements with a single profile system in a tall-dense-canopy temperate forest. Agr Forest Meteorol 228-229: 327-338.
https://doi.org/10.1016/j.agrformet.2016.07.020

Wang, X, Wang C, Li Q (2015) Wind regimes above and below a temperate deciduous forest canopy in complex terrain: Interactions between slope and valley winds. Atmosphere-Basel 6(1): 60-87.
https://doi.org/10.3390/atmos6010060

Warton DI, Wright IJ, Falster DS, et al. (2006) Bivariate line-fitting methods for allometry. Biol Rev 81(2): 259-291.
https://doi.org/10.1017/S1464793106007007

Weiss A, Norman JM (1985) Partitioning solar radiation into direct and diffuse, visible and near-infrared components. Agr Forest Meteorol 34(2): 205-213.
https://doi.org/10.1016/0168-1923(85)90020-6

Whiteman CD, Allwine KJ, Fritschen LJ, et al. (1989) Deep valley radiation and surface energy budget microclimates. Part I: Radiation. J Appl Meteorol 28(6): 414-426.

Wilson K, Goldstein A, Falge E, et al. (2002) Energy balance closure at FLUXNET sites. Agr Forest Meteorol 113(1-4): 223-243.
https://doi.org/10.1016/S0168-1923(02)00109-0

Wohlfahrt G, Hammerle A, Niedrist G, et al. (2016) On the energy balance closure and net radiation in complex terrain. Agr Forest Meteorol 226: 37-49.
https://doi.org/10.1016/j.agrformet.2016.05.012

Xu K, Xing Y, Chang X (2021) Model optimization and gpp estimation of light energy utilization in subtropical evergreen coniferous forest. For Eng 37(1): 28-36. (In Chinese)
https://doi.org/10.16270/j.cnki.slgc.2021.05.013

Yan H, Wang S, Dai J, et al. (2021) Forest greening increases land surface albedo during the main growing period between 2002 and 2019 in China. J Geophysical Res-Atmos 126(6): e2020JD033582.
https://doi.org/10.1029/2020jd033582

Yang D (2016) Solar radiation on inclined surfaces: Corrections and benchmarks. Sol Energy 136(Supplement C): 288-302.
https://doi.org/10.1016/j.solener.2016.06.062

Zitouna-Chebbi R, Prévot L, Jacob F, et al. (2012) Assessing the consistency of eddy covariance measurements under conditions of sloping topography within a hilly agricultural catchment. Agr Forest Meteorol 164: 123-135.
https://doi.org/10.1016/j.agrformet.2012.05.010